6th IEEE RAS/EMBS International Conference on
Biomedical Robotics and Biomechatronics (BioRob)
June 26-29, 2016. UTown, Singapore

A Constrained Extended Kalman Filter For Dynamically Consistent Inverse Kinematics and Inertial Parameters Identification

V. Bonnet, G. Daune, V. Joukov, R. Dumas, P. Fraisse, D. Kulić, A. Seilles, S. Andary, G. Venture

Abstract— **This paper presents a method for the real-time determination of joint angles, velocities, accelerations and joint torques of a human. The proposed method is based on a constrained Extended Kalman Filter that combines stereophotogrammetric and dynamometric data. In addition to the joint variables, subject-specific segment lengths and inertial parameters are identified. Constraints are added to the filter, by restricting the optimal Kalman gain, in order to obtain physically consistent parameters. An optimal tuning procedure of the filter's gains and a sensitivity analysis is presented. The method is validated in the plane on four human subjects and shows very good tracking of skin markers with a RMS difference lower than 15 mm. External ground reaction forces and resultant moment are also accurately estimated with an RMS difference below 3 N and 6 N.m, respectively.**

I. Introduction

THE dynamics state of a branched kinematic system such as a human or a humanoid is characterized by the joint and segment position, velocity and acceleration vectors and also by the internal and external wrenches acting on the body. Estimating these is of crucial importance in countless applications related to robotics, orthopaedics or industrial ergonomics. Stereophotogrammetric and force-plate systems are usually used to quantify human motion. An accurate, real time method able to provide physically consistent kinematics and dynamics variables would be a great advantage in various applications. In robotics, real-time ability is essential when a robot must react at each sample of time accordingly to the dynamics current state of the human being. An improve accuracy is also desirable when designing or adapting to a subject prosthetics and exoskeletons. Numerous approaches have been proposed to estimate human motion from marker trajectories and force-plate data [1]. The most classical approach is to create a frame at each segment from the markers, and to calculate the relative linear and angular displacements between adjacent frames. Despite its ease of use, this method does not take advantage of kinematics constraints and is very sensitive to several sources of error, such as marker misplacements and soft tissue artifacts [2-5]. Soft tissue artifacts are highly non-linear and are caused by motion of the skin or by wobbling masses jeopardizing, by as much as 15 degrees, the estimate of the underlying bone pose [3]. Model based approaches, inspired from robotics filed, combining marker trajectories and a kinematics model with fixed segment lengths have been presented [6-8] and are now used in several commercial software products [9]. These are referred in biomechanics as *global optimization techniques* [6-7]. They usually attempt to minimize, at each sample of time, the least square difference between the measured and model-predicted marker positions for all the segments at the same time while respecting biomechanical constraints. These multi-body approaches have shown better accuracy than treating the segments separately [6][10-11]. However, they do not consider the history of the marker trajectories and are computationally expensive excluding *de-facto* real-time applications. Recently, the Extended Kalman Filter (EKF) has been used to overcome some of these issues and has been shown to have better performance than global optimiza-tion [10-11]. The use of EKF allows joint angles to be smoothed and reduces the effect of skin artifacts [10-11]. Reduced noise velocity and acceleration estimates enable a much better estimate of internal joint loads and recon-struction of ground reaction forces and moments (GRFM). However, to the best of our knowledge, no study has investigated the use of EKF for reconstructing dynamic quantities. Additionally, almost all of the stud-ies use averaged anthropometric tables (AT) obtained from cadaver data to estimate body segment inertial pa-rameters (BSIP) [12-13]. The use of AT for joint torque estimates becomes problematic when dealing with indi-viduals characterized by an atypical body mass distribu-tion. Recently, inspired by the robotics field of system identification, Ayusawa et al. [14] have proposed several approaches for identifying human BSIP using offline least-square identification and quadratic optimisation methods collected over a calibration phase. These meth-ods have shown the possibility of using the GRFM and the general dynamics equation of a floating base system to identify each BSIP [13]. The major differences be-tween human and robot are that the joint trajectories can be measured accurately, the segments are perfectly rigid and that the joint torques can often be measured in a robot. This latter quantity can then be used in the identi-fication process instead of the external wrench. This was done recently by Joukov et al. [15] who proposed a con-strained EKF to identify in real-time inertial parameters of a serial manipulator robot [15] using measurements of robot joint encoder and torque sensors.

In this context, a new tool merging previous studies from

V. Bonnet, G. Daune, and G. Venture are with the department of mechanical systems engineering, Tokyo University of Agriculture and Technology, Japan. (e-mail: bonnet.vincent@gmail.com).

V. Joukov and D. Kulić are with the department of electrical and computer engineering, University of Waterloo, Waterloo, ON, Canada.

R. Dumas is with the LBMC UMR T9406, University of Lyon – IFSTTAR, Lyon, France.

P. Fraisse is with LIRMM UMR 5506 CNRS, University of Montpellier, Montpellier, France.

A. Seilles and S. Andary are with NaturalPad, Montpellier, France.

both biomechanics and robotics is proposed in or-der to perform a dynamically consistent inverse kinematics. The contribution of this paper are:

- an accurate real-time estimate of joint positions, velocities, accelerations and joint torques of a human,
- a modified EKF gain constraint that constrains the identification of segment lengths and inertial parameters to physically feasible values,
- a detailed and pragmatic method for tuning the measurement and process covariance matrices of the EKF.

Unlike previous studies, data obtained from kinematics and dynamometric measurements are used together in the same EKF filter to estimate the above mentioned quantities.

II. METHOD

A. A. *The squat exercise*

In order to exemplify the proposed approach a popular planar squat rehabilitation exercise was chosen. Squat exercises are widely used in rehabilitation programs [16], since they allow the evaluation of basic skills of daily living, such as picking up an item, navigating stairs, or sit-to-stand transfer. The experimentation involved four young healthy volunteers (2 males, 2 females, age=33±5 years, mass=71±3 kg, height=1.72 ± 0.04 m). Starting from their natural standing posture, volunteers were asked to perform a squatting task, moving at a self-selected speed, to reach a lower position of their choice and then return to their initial posture. The task was composed of two series of 10 repetitions. A force plate (*Bertec Inc*) was used to record GRFM, and a stereophotogrammetric system (*9 Mx cameras, VICON*) simultaneously recorded marker trajectories. Twelve reflective markers were located on one side of the subject according to the popular Plug-In-Gait (VICON) marker template (Fig.1). Each marker was associated to a body segment. Since the squat task is planar, the joint angles were calculated in accordance with the literature between adjacent vectors created from marker positions [1]. The resultant joint angles were used for comparison with our method.

B. *The mechanical model*

A mechanical model of the squat exercise was created using a 7-segment planar model (Fig.1). Segments were connected by cylindrical hinges $\boldsymbol{\theta}=[\theta_1\ \theta_2\ \theta_3\ \theta_4\ \theta_5\ \theta_6\ \theta_7]^T$ representing (Fig. 1). The origin of the global system of reference ($^GX^GY$) was located on the tip of the toe, which was assumed to be stationary during the exercise. For the sake of simplicity and because it provides symbolic equations, the Modified Denavit-Hartenberg notation [17] and the SYMORO+ [18] software were used to formulate the kinematic and inverse dynamics model. Joint center positions can be estimated in the global reference frame using the forward kinematics model as a function of the joint angles and the segment lengths. Moreover, the position of the markers in the global reference frame can be computed using the same forward kinematics model and the rigid transformation of the local coordinates ($^lp_{mkx}$, $^lp_{mky}$) of each marker in their corresponding joint frame (Fig.1).

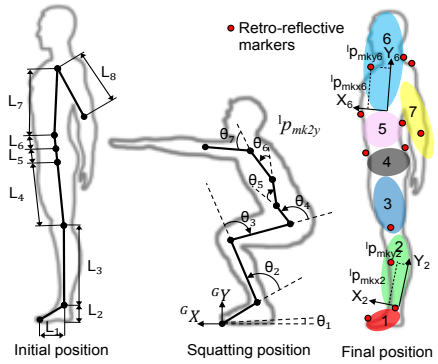

Fig.1. Seven-degree-of-freedom model of the human body.

The inverse dynamics model of the body system is computed with Lagrange's equations:

$$\boldsymbol{\Gamma} = \boldsymbol{A}(\boldsymbol{q})\ddot{\boldsymbol{q}} + \boldsymbol{C}(\boldsymbol{q},\dot{\boldsymbol{q}})\dot{\boldsymbol{q}} + \boldsymbol{G}(\boldsymbol{q}) + \boldsymbol{J}^T\boldsymbol{F} \quad (1)$$

where $\boldsymbol{q},\dot{\boldsymbol{q}},\ddot{\boldsymbol{q}},\boldsymbol{\Gamma}$ are respectively the vectors containing the joint position, velocity, acceleration and torque components. $\boldsymbol{A}$, $\boldsymbol{C}$, $\boldsymbol{G}$ are the inertia, Coriolis and centrifugal, and gravity matrices, respectively. $\boldsymbol{J}$ is the Jacobian matrix mapping $\boldsymbol{F}=[F_X\ F_Y\ M_Z]^T$ the vector of the external wrench to the joint space. The i^{th} segment of the mechanical model has a mass M_i, a moment of inertia around the z-axis ZZ_i and two components of the first moment of inertia (MX_i, MY_i).

C. *Extended Kalman Filter*

The aim of the proposed EKF is to estimate at the same time:

- joint angles,
- joint velocities,
- joint accelerations,
- segment lengths and local marker positions,
- and the body segments inertial parameters,

by tracking the marker trajectories and each component of the measured external wrench. The system overview is illustrated in Fig. 2.

1) EKF formulation

The EKF is a common sensor fusion algorithm used to estimate the state of a non-linear system given noisy measurements by minimizing the trace of the error covariance matrix $\boldsymbol{P}$. The EKF uses a linear approximation computed at every iteration. The next state estimate $\boldsymbol{x}_{k+1}$ and measurement update $\boldsymbol{y}_{k+1}$ are defined by:

$$\begin{aligned}\boldsymbol{x}_{k+1} &= f(x_k) + \boldsymbol{w}_k \\ \boldsymbol{y}_{k+1} &= h(x_k) + \boldsymbol{v}_k\end{aligned} \quad (2)$$

where f and h are the functions relating the previous step to the next step and the state vector to the measurement vector, respectively. $\boldsymbol{w}$ and $\boldsymbol{v}$ represent the process and the measurement Gaussian noise with zero mean and covariance $\boldsymbol{Q}_k$ and $\boldsymbol{R}_k$, respectively.

As shown in Fig.2, the objective of the EKF is to produce the best estimate of the state vector that minimises the least-square difference between the measured and estimated $\boldsymbol{y}$ vector trough a two steps prediction-update procedure.

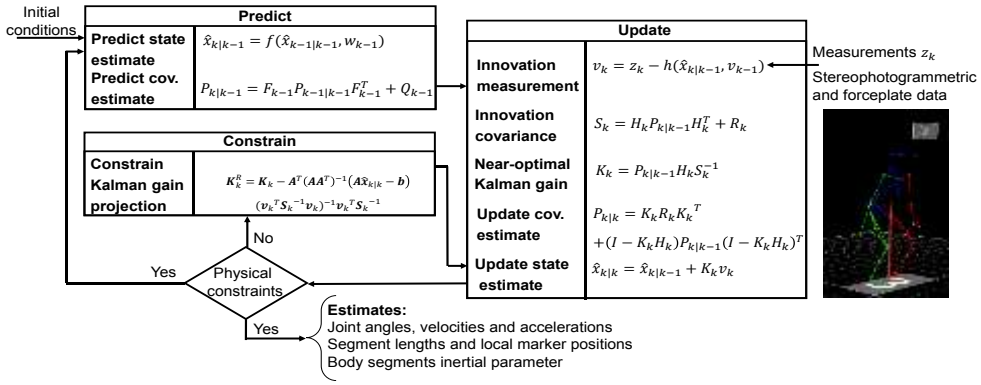

Fig. 2. Overview of the constrained extended Kalman filter.

In Fig. 2, $\hat{\boldsymbol{x}}_{k|k}$, $\boldsymbol{P}_{k|k}$ and $\boldsymbol{K}_k$ are the predicted mean and covariance of the state vector and the EKF gain matrix, respectively. **H** and **F** are the Jacobian matrices of *f* and *h* calculated symbolically relatively to the state vector.

2) EKF state and measurement vectors

The state vector required to estimate the human body dynamics is as follows:

$$\boldsymbol{x}_{i=1:7} = [\theta_i\ \dot{\theta}_i\ \ddot{\theta}_i\ \ L_i\ \ {}^lP_{xi}\ \ {}^lp_{yi}\ M_i\ MX_i\ MY_i\ ZZ_i]^T \qquad (3)$$

The state update equation assumes that the joint variables evolve linearly and that the other parameters are constants. Thus for each frame *i* carrying *j* markers, it is defined as follows:

$$\begin{bmatrix} \theta_{ik} \\ \dot{\theta}_{ik} \\ \ddot{\theta}_{ik} \\ L_{ik} \\ p_{x,j\,k} \\ p_{y,j\,k} \\ M_{ik} \\ MX_{ik} \\ MY_{ik} \\ ZZ_{ik} \end{bmatrix} = \begin{bmatrix} \begin{bmatrix} 1 & \Delta t & \frac{\Delta t^2}{2} \\ 0 & 1 & \Delta t \\ 0 & 0 & 1 \end{bmatrix} & O_{3x7} \\ O_{7x3} & I_{7x7} \end{bmatrix} \begin{bmatrix} \theta_{ik-1} \\ \dot{\theta}_{ik-1} \\ \ddot{\theta}_{ik-1} \\ L_{ik-1} \\ p_{x,j\,k-1} \\ p_{y,j\,k-1} \\ M_{ik-1} \\ MX_{ik-1} \\ MY_{ik-1} \\ ZZ_{ik-1} \end{bmatrix} \qquad (4)$$

where Δt is the time difference between samples.

The measurement vector at each time step k is composed of the 2D marker trajectories, each component of the external wrench vector, and the total mass of the subject, previously measured.

$$\boldsymbol{z}_k = [\ {}^Gp_{mkxjk}\ \ {}^Gp_{mkyjk} \dots F_{Xk}\ F_{Yk}\ M_{Zk}\ \textstyle\sum_{i=1}^{7} M_i]^T \qquad (5)$$

The total mass is used as a soft constraint [19] with a very small measurement process noise in order to force the sum of the all the masses to be of a fixed value.

3) EKF constraints

In order to ensure physical consistency of some of the state vector parameters, inequality constraints must be added to the EKF. A method presented by Gupta et al. [20], allows constraints to be easily implemented on the state vector elements, has been used and modified. It proposes to restrict the optimal Kalman gain in a way that the updated state estimate lies within the constrained space. The following constraints can be implemented using this method:

$$\begin{cases} A_{KF}\hat{x}_{k|k} = b \\ C_{KF}\hat{x}_{k|k} \le d \end{cases} \qquad (6)$$

However, the method presented for inequality constraints requires the use of an optimization process that is not suitable for real-time application [19-20]. Therefore, Gupta et al.'s method was adapted as follows: At each timestep, an initial Kalman gain and state update are computed, then if one of the elements of the updated state vector is over its limits, a vector of constraints $\boldsymbol{b}$ is filled at the corresponding row with the limit of this element of the state vector. Using the vector of constraints and the updated state vector a new optimal Kalman gain is then computed as follows:

$$\boldsymbol{K}_k^R = \boldsymbol{K}_k - \boldsymbol{A}_{KF}^T(\boldsymbol{A}_{KF}\boldsymbol{A}_{KF}^T)^{-1}(\boldsymbol{A}_{KF}\hat{\boldsymbol{x}}_{k|k} - \boldsymbol{b})(\boldsymbol{v}_k{}^T\boldsymbol{S}_k{}^{-1}\boldsymbol{v}_k)^{-1}\boldsymbol{v}_k{}^T\boldsymbol{S}_k{}^{-1} \qquad (7)$$

Finally the update of the state vector can be computed using this new Kalman gain.

$$\hat{\boldsymbol{x}}_{k|k}^R = \hat{\boldsymbol{x}}_{k|k} + \boldsymbol{K}_k^R\boldsymbol{v}_k \qquad (8)$$

Using this technique it is possible to constrain the parameters and the joint angles to stay within physically consistent limitations. Geometrical, inertial parameters and joint angle limits were set using the biomechanics literature [12]. The segment lengths and inertial parameters were set arbitrarily to be within 20 % of their literature value. The maximal and minimal local positions of the markers were tuned manually to constrain the marker positions to lie within the segments. The following set of constraints has been implemented:

$$\begin{cases} \theta_{imin} < \theta_i < \theta_{imax} \\ L_{AT} - 0.2L_{AT} \le L \le L_{AT} + 0.2L_{AT} \\ -Treshold \le {}^lp_{mkx} \le Treshold \\ -Treshold \le {}^lp_{mky} \le Treshold \\ M_{AT} - 0.2M_{AT} \le M \le L_{AT} + 0.2M_{AT} \\ MX_{AT} - 0.2MX_{AT} \le MX \le MX_{AT} + 0.2MX_{AT} \\ MY_{AT} - 0.2MY_{AT} \le MY \le MY_{AT} + 0.2MY_{AT} \\ ZZ_{AT} - 0.2ZZ_{AT} \le ZZ \le ZZ_{AT} + 0.2ZZ_{AT} \end{cases} \qquad (9)$$

where the index AT refers to the anthropometric tables [12].

4) EKF parameter tuning

The Extended Kalman filter requires parameter tuning to guarantee stability while maximizing convergence rate over a given task [21]. The parameters that may be used to tune the behavior of the algorithm are embodied in the process covariance matrix **Q** and in the measurement covariance matrix **R**. Since our EKF deals with multiple degree-of-freedom and different quantities several gains are to be tuned. The measurement covariance matrix **R** has not been set using directly the measurement noise of the stereophotogrammetric system (about 1mm). Indeed, the literature in biomechanics proposes quantitative tables describing the influence of the soft-tissue artifacts on the relative displacement between the marker and the underlying segment [3-5]. Consequently, these tables appear to be a better indicator on how reliable is the measurement of each specific marker for the estimate of the segment pose. For the force-plate data the noise measurement provided by the manufacturer was used. The values of **R** are given in Table I. For the process covariance matrix **Q**, there is no real consensus, and no real data, in the literature on how to tune its parameters. Since the segment lengths and inertial parameters are independent parameters and it is desirable that they converge to a constant value, the diagonal elements of Q corresponding to them can be set to zero. This guarantees that the error covariance ***P*** matrix will also eventually converge to zero for those terms and thus that the state will not be dependent on the measurement [22].

The process noise corresponding to the position of the marker in the local frame was set for the same reason to a small value ($1e^{-4}$). However, local maker positions might slightly evolve due to the soft-tissue artifacts creating an actual displacement between a marker and its corresponding local frame. Process gains related to the evolution of joint angles (Q_q), velocities ($Q_{\dot{q}}$) and accelerations ($Q_{\ddot{q}}$) should be much larger since these variables are supposed to evolve in time and also to reflect the errors due to the linear assumption of the model (eq.4). A numerical tuning based on the experimental data was devised to tune these parameters. The optimal combination of these gains was determined through an iterative process that sought the minimal value of the sum of the RMS difference between estimated and measured markers and GRFM. The coefficients were varied through all possible combinations from $1e^{-6}$ to $1e^{6}$ on a logarithmic scale. A trial that was not used in the assessment of the method accuracy was selected to perform the optimal gain tuning. Fig. 3 presents the sensitivity analysis to the filter's process noise gains. Several gain combinations lead to filter instabilities and thus no values are displayed. These instabilities occur mainly when Q_q, and $Q_{\dot{q}}$ are very small. This might reflect the error in the constant acceleration assumption in the state update. Consequently, the lowest values of the sum of all RMS (plotted in red) were obtained for all the combinations in which all the gains are of large value. Among these combinations, the optimal solution was the one obtained for $Q = 1e^3$, $Q_{\dot{q}} = 1e^2$, $Q_{\ddot{q}} = 1e^3$. Anthropometric table values [12] and the distances between markers at the first time step were used to set the initial condition of the filter.

III. Results

Fig.4 shows a representative tracking of the markers and segment lengths for a randomly chosen subject over a complete squat cycle. Fig. 5 shows a comparison between the joint angles estimated by the proposed EKF method and by the *reference* marker method (see section II.A).

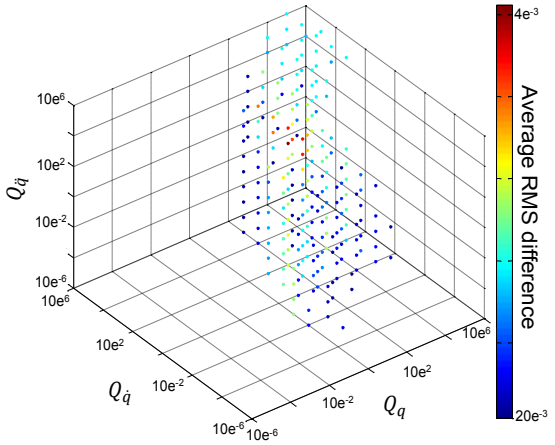

Fig. 3. Sum of RMS difference as a function of the values of the coefficients $\boldsymbol{Q}$, $\boldsymbol{Q_{\dot{q}}}$, and $\boldsymbol{Q_{\ddot{q}}}$ on a logarithmic scale. Results refer to the 10 squats of a randomly chosen subject.

TABLE I
MEASUREMENT (**R**) AND PROCESS (**Q**) MATRICES GAINS VALUES

	Value	Description	Method
R_{TOE}	$1e^{-3}$	Toe marker	[3]
R_{ANK}	$10e^{-3}$	Ankle marker	[3]
R_{SHA}	$15\ e^{-3}$	Shank marker	[3]
R_{KNE}	$30e^{-3}$	Knee marker	[3]
R_{ASIS}	$17e^{-3}$	Pelvis markers	[5]
R_{T10}	$10.7e^{-3}$	T10 marker	[4]
R_{STRN}	$15e^{-3}$	Sternum marker	[4]
R_{SHO}	$10e^{-3}$	Acromion marker	[4]
R_{FX}	0.1	Horizontal GRF	manufacturer
R_{FY}	0.1	Vertical GRF	manufacturer
R_{MZ}	0.1	Ground resultant couple	manufacturer
R_{Mtot}	$1e^{-4}$	Mass soft constraint	empiric
Q_θ	$1e^{3}$	Joint angle	Identified
$Q_{\dot{\theta}}$	$1e^{2}$	Joint velocity	Identified
$Q_{\ddot{\theta}}$	$1e^{3}$	Joint acceleration	Identified
Q_L	0	lengths and inertial param	[22]
Q_p	$1e^{-4}$	Local marker coordinates	empiric

The question of the formal validation of any inverse kinematics method for humans is still an open issue. In fact, no estimation method can be qualified as the gold standard for any type of movement. The only measurements being the marker positions and GRFM, other studies usually propose to analyse the RMS residue of the tracking of the markers [10-11] and the RMS differences between estimated and measured GRFM. Consequently, in this paper the proposed method is validated similarly by a direct comparison between the measured and estimated quantities. The RMS difference, normalized RMS (NRMS) difference and the correlation coefficient (r) were calculated. As indicated by Table II, showing the results obtained during all the 80 squats, the proposed algorithm was able to track very accurately the marker trajectories, and the GRFM with RMS differences lower than 13 mm, 1 N, 3 N, and 6 Nm, respectively. The highest differences in markers tracking was always obtained

for the sternum marker. The combined use of AT and joint trajectories calculated directly from markers do not provide an accurate estimate of the external wrench components with a NRMS at least 10 times higher than when using the proposed EKF method. This is exemplified by Fig. 6 that shows the typical behavior of the proposed method: after a short adaptation time (2s), the proposed algorithm is able to track, very accurately, GRFM recorded during the squat exercise.

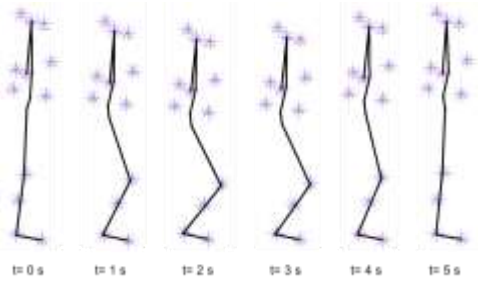

Fig. 4 Representative results showing the very good estimation (blue stars) of the measured (red triangles) markers during a whole squat cycle.

TABLE II
RESULTS OF THE TRACKING OF THE RETRO-REFLECTIVE MARKERS AND COMPARISON OF THE ESTIMATE OF THE GROUND REACTION FORCES AND RESULTANT MOMENTS.

		RMS	NRMS	CC
mk_{TOE}		0±0	0±0	1±0
mk_{ANK}		2.7±0.4	3.9±0.8	0.74±0.10
m_{SHA}		7.4±1.1	4.1±1.0	0.82±0.12
m_{KNE}		7.3±0.8	5.1±1.1	0.99±0.01
m_{ASIS}		9.7±2.3	13.6±8.9	0.95±0.03
m_{T10}		7.5±2.1	2.3±0.4	0.93±0.04
m_{STRN}		13.0±2.2	34.8±14.0	0.77±0.10
m_{SHO}		9.0±2.1	8.2±2.2	0.94±0.03
FX	EKF	0.6±0.3	21.5±10.1	0.97±0.02
	AT	10.8±6.3	111.1±8.8	0.10±0.18
FY	EKF	2.2±1.3	0.31±0.1	0.99±0.01
	AT	15.3±9.3	2.2±1.2	0.96±0.02
MZ	EKF	5.6±1.3	7.8±2.4	0.90±0.06
	AT	14.8±6.8	77.7±6.4	0.66±0.08

On this figure the corresponding RMS errors were for F_X, F_Y and M_Z: AT(11 N, 10 N, 16 N.m) and EKF(1 N, 2 N, 6 N.m). These differences might lead to dramatically bad estimate of the joint torques. Fig.7 shows this influence on a representative estimate of the knee joint torque during a squat. In this figure the RMS difference between the two estimates is of 12 N.m or 20 % when normalized. Differences observed over dynamic variables might be explained by the joint kinematics but also by the value of the inertial parameters. As previously discussed inertial parameters have a non-negligible influence when performing inverse dynamics. Figs. 8 and 9 present the evolution of the segment lengths, segment masses and of the segment inertias. The first moment of inertias were not displayed since in our data they stay very close to the ones estimated with AT. The segment lengths and segment masses evolve rapidly at the beginning of the task, as highlighted in Fig. 7, and converge toward a fixed value.

IV. DISCUSSION

The marker residual of the present study is less than 15 mm and the tracking of each of the external wrench components was excellent (NRMS 20 %) compare to the classical one (NRMS 110%).

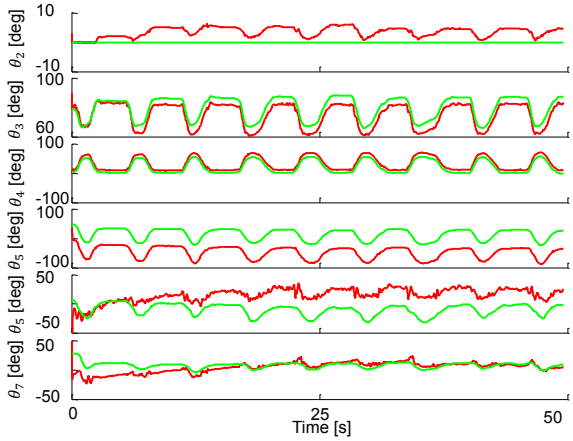

Fig. 5. Representative results showing the comparison between EKF joint angles (red lines) and the so-called classical method (green lines).

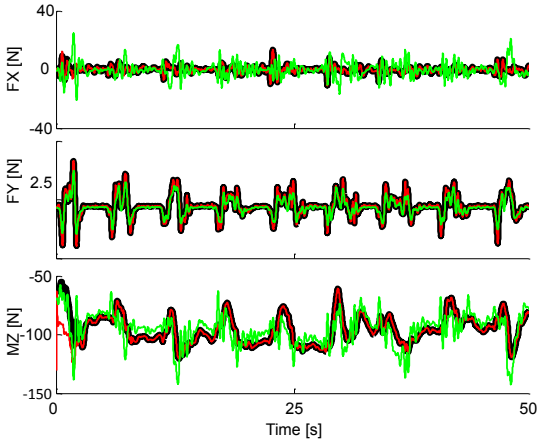

Fig. 6. Representative results showing the measured (black lines), the EKF estimate (red lines) and the AT estimate (green lines) of the external wrench components.

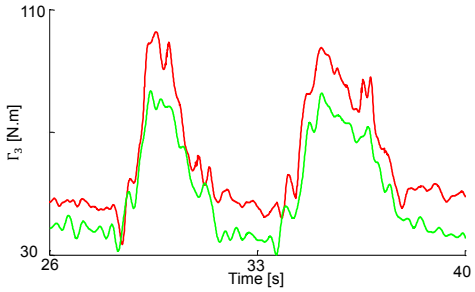

Fig. 7. Comparison of the EKF estimate (red lines) and of the AT estimate (green lines) of the joint torque of the knee.

The marker residual is similar to existing studies in the literature [11] and can be explained by the influence of soft-tissue artifacts since instrumental errors influencing the 3D marker reconstruction can be assumed to be negligible [11].

The real-time reconstruction of the GRFM is better than in a previous study of our group that was using an off-line method [13] over a similar squat task. However, the identification was previously performed using low-cost sensors. Further investigation should be done to compare our method with more advanced global optimization methods and commercial software [7-9]. However, there is a serious lack in the literature on how the weight of each marker should be tuned during the inverse kinematics process and on how differences in model definition, movement of interest, impact the marker residuals. Indeed, the tuning of the algorithm parameters largely affects the final results [11]. To address this shortcoming, the present study proposes a pragmatic methodology to tune the measurement and process covariance matrices gains. Uniquely, our method allows us also to track the dynamic evolution of segment masses and BSIP quantities. This can be beneficial during a rehabilitation process or during the evaluation of an assistive device. For example, the tracking of the evolution of a specific segment mass can help the clinician to focus a muscular reinforcement program on a given muscle [13]. The BSIP values presented in this study do not strongly evolve from their AT values. This can be due to the fact that the solution is not unique. Indeed, it is possible that some of the BSIP regroup themselves in the so-called base-parameters [13][15].

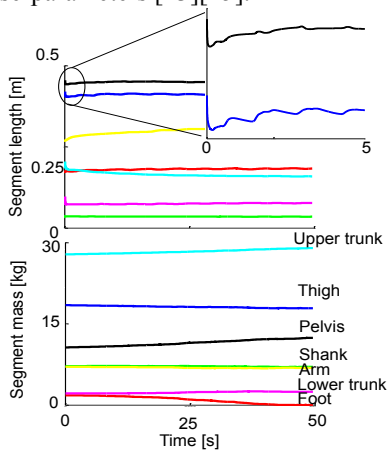

Fig. 8. Representative results showing the estimation of the segment lengths and masses during the squat exercise. The colors of the lines correspond to the ones of the segments displayed in Fig.1.

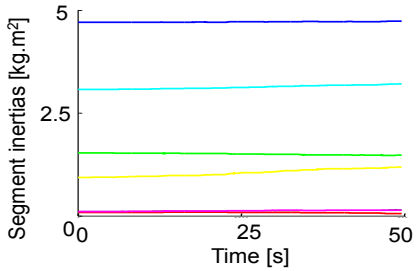

Fig. 9. Representative results showing the estimation of the segment inertias during the squat exercise.

ACKNOWLEDGEMENT

This study was supported by the Japan Society for Promotion of Science (No PE13559).

V. REFERENCES

[1] A. Cappozzo, F. Catani, U.D. Croce, A. Leardini, Position and orientation in space of bones during movement : anatomical frame definition and determination," *Clin. Biomech.*, vol.10, pp.171-178, 1995.

[2] R. Dumas, E. Nicol, L. Cheze, "Influence of the 3D inverse dynamic method on the joint forces and moments during gait," *J. of Biomech. Eng.*, vol. 129, pp. 786-790, 2007.

[3] A. Peters, B. Galna, M. Sangeux, M. Morris, R. Baker, "Quantification of soft tissue artifact in lower limb human motion analysis: A systematic review", *Gait & Posture*, vol. 31, pp 1-8, 2010.

[4] R. Zemp, R. List, T. Gülay, J.P. Elsig, J. Naxera, W.R. Taylor, S. Lorenzetti,"Soft Tissue Artefacts of the Human Back: Comparison of the Sagittal Curvature of the Spine Measured Using Skin Markers and an Open Upright MRI", *Plos One*, vol.9, 2014.

[5] R. Hara, M. Sangeux, R. Baker, J. McGinley, "Quantification of pelvic soft tissue artifact in multiple static positions", *Gait & Posture*, vol. 39, pp 712-717, 2014.

[6] T.W. Lu, JJ. O'Connor, "Bone position estimation from skin marker co-ordinates using global optimisation with joint constraints," *J. Biomech.*, pp. 129-134, 1999.

[7] J.A. Reinbolt, J.F.Schutte, B.J. Fregly, B. Koh, R.T. Haftka, A.D. George, K. Mitchell, "Determination of patient-specific multi-joint kinematic models through two-level optimization", *J. Biomech.*, vol. 38, pp. 621-626, 2005.

[8] M.S. Andersen, M. Damsgaard, J. Rasmussen, "Kinematic analysis of over-determinate biomechanical systems," *Comput Methods Biomech Biomed Engin*., vol. 12, pp. 371-84, 2009.

[9] S.L. Delp, F.C. Anderson, A.S. Arnold, P. Loan, A. Habib, C.T. John, E. Guendelman, D.G. Thelen, "OpenSim open-source software to create and analyze dynamic simulations of movement," *IEEE Trans. Biomed. Eng.*, vol. 54, pp. 1940-1950, 2007.

[10] P. Cerveri, A. Pedotti, G. Ferrigno, "Kinematics models to reduce the effect of skin artifacts on markerbased human motion estimation", J. Biomech. Vol. 38, pp. 2228–2236, 2005.

[11] V. Fohanno, M. Begon, P. Lacouture, F. Colloud, "Estimating joint kinematics of a whole body chain model with closed-loop constraints", *Mult. Sys. Dyn*., vol. 31, pp.433-449, 2014.

[12] R. Dumas, L. Chèze, J. Verriest, "Adjustments to McConville et al. and Young et al. body segment inertial parameters," *J. Biomech.*, vol. 40, 2007, pp. 543–553.

[13] V. Bonnet, G. Venture, "Fast determination of the planar body segment inertial parameters using affordable sensors", *IEEE Trans. Biomed. Eng.*, vol.23, pp. 628-635, 2015.

[14] K. Ayusawa, G. Venture and Y. Nakamura, **"**Identifiability and Identification of Inertial Parameters Using the Underactuated Base-Link Dynamics for Legged Multibody Systems," *Int. J. Robot. Res.*, 2013.

[15] V. Joukov, V. Bonnet, G. Venture, D, Kulic, "Constrained dynamic parameter estimation using the extended Kalman filter", *IEEE Int. Conf. Robot and Sys.*, Hamburg, Germany, accepted for publication, 2015.

[16] V. Bonnet, C. Mazza, P. Fraisse, A. Cappozzo, "A least-square identification algorithm for estimating squat exercise mechanics using a single inertial measurement unit," *J. Biomech*., vol. 45, pp. 1472-1477, 2012.

[17] W. Khalil, and E. Dombre, "Modeling, identification and control of robots," *Eds. Hermès Penton*, London, United Kingdom, 2002.

[18] W. Khalil and D. Creusot ", SYMORO+: A system for the symbolic modeling of robots," *Robotica*, pp.153-161, 2008.

[19] D. Simon, "Kalman filtering with state constraints: a survey of linear and nonlinear algorithms," *IET Control Theory Appl.*, pp. 1–16, 2009

[20] N. Gupta, R. Hauser, "Kalman filtering with equality and inequality state constraints," *Arxiv*, http://arxiv.org/abs/0709. 2791, 2009.

[21] C. Mazzà, M. Donati, J. McCamley, P. Picerno, and A. Cappozzo, "An optimized Kalman filter for the estimate of trunk orientation from inertial sensors data during treadmill walking", *Gait & Posture*, vol. 35, pp. 138-142, 2011.

[22] B. Southall, B.F. Buxton, J.A. Marchant, "Controllability and observability: Tools for Kalman filter design," *In Proc. British machine Conf.*, pp. 17.1-17.10, 1998.